



Available online at [www.sciencedirect.com](http://www.sciencedirect.com)

ScienceDirect



RESEARCH ARTICLE

## Characterization of volatile organic compounds in grafted tomato plants upon potyvirus necrotic infection



Roberta SPANÒ<sup>1</sup>, Mariarosaria MASTROCHIRICO<sup>1</sup>, Francesco LONGOBARDI<sup>2#</sup>, Salvatore CERVELLIERI<sup>3</sup>, Vincenzo LIPPOLIS<sup>3</sup>, Tiziana MASCIA<sup>1#</sup>

<sup>1</sup> Department of Soil, Plant and Food Sciences, University of Bari “Aldo Moro”, Via Amendola 165/A, Bari 70126, Italy

<sup>2</sup> Department of Chemistry, University of Bari “Aldo Moro”, Via Orabona 4, Bari 70126, Italy

<sup>3</sup> National Research Council (CNR), Institute of Sciences of Food Production (ISPA), Via Amendola 122/O, Bari 70126, Italy

### Abstract

A headspace solid-phase microextraction-gas chromatography-mass spectrometry (HS-SPME/GC-MS) method was used to study the volatile organic compounds (VOCs) associated with the differential immune response of tomato plants infected with the recombinant strain of potato virus Y (PVY<sup>C-to</sup>), necrogenic to tomato. Analysis was carried out in UC82 (UC), a virus susceptible tomato variety, comparing the same UC plants grafted or not onto a virus tolerant tomato ecotype, Manduria (Ma); the three types of samples used for the GC-MS analysis were mock-inoculated UC/Ma plants, UC/Ma+PVY<sup>C-to</sup> and UC+PVY<sup>C-to</sup> plants; the VOCs obtained were 111. Results from symptomatic PVY<sup>C-to</sup>-infected UC plants showed a VOCs composition enriched in alcohols, fatty acid derivatives, benzenoids, and salicylic acid derivatives, while in mock-inoculated UC/Ma plants VOCs were mainly characterized by methyl ester compounds. The VOC profile was in line with RNAseq data analyses, denoting that PVY<sup>C-to</sup> viral RNA accumulation and disease symptoms induce the specific transcriptional activation of genes involved in VOCs biosynthesis. Furthermore, principal component analysis highlighted that VOCs of PVY<sup>C-to</sup>-infected and mock-inoculated grafted plants were much closer each other than that of symptomatic PVY<sup>C-to</sup>-infected non-grafted UC plants. These results suggest that VOCs profiles of tomato plants are related to the viral RNA accumulation, disease intensity and graft-derived tolerance to PVY<sup>C-to</sup> infection.

**Keywords:** tomato, potyvirus, VOCs, defense, grafted plants

## 1. Introduction

Plants and fruits emit specific biogenic volatile organic compounds (VOCs) in response both to pathogens and herbivore insect attacks, thus resulting in indirectly induced defense responses (Beck *et al.* 2008, 2009; Erb *et al.* 2012; Sharma *et al.* 2019; Deng *et al.* 2021; Dong *et al.* 2022; Lin *et al.* 2022). Beneficial root-colonizing microbiomes altering the VOCs bouquet can expand such defense response by attracting or favouring the activity of parasitoids and predators of herbivore insects

Received 1 September, 2022 Accepted 26 January, 2023  
Roberta SPANÒ, E-mail: [roberta.spano@uniba.it](mailto:roberta.spano@uniba.it);  
#Correspondence Francesco LONGOBARDI, Tel: +39-0805442042, E-mail: [francesco.longobardi@uniba.it](mailto:francesco.longobardi@uniba.it); Tiziana MASCIA, Tel: +39-0805442913, E-mail: [tiziana.mascia@uniba.it](mailto:tiziana.mascia@uniba.it)

© 2023 CAAS. Published by Elsevier B.V. This is an open access article under the CC BY-NC-ND license (<http://creativecommons.org/licenses/by-nc-nd/4.0/>).  
doi: 10.1016/j.jia.2023.02.032

on different plant species, including tomato (Battaglia *et al.* 2013). Besides the plant damage induced by trophic activity, some herbivore insects can also transmit viruses, which, in turn, change/modify VOCs emission in order to promote virus spread. Indeed, VOCs seem to be directly related to the non-persistent or persistent mode of the viral transmission (Eigenbrode *et al.* 2018; Carr *et al.* 2019). The attractiveness of *Cucurbita pepo* to *Myzus persicae* and *Aphis gossypii*, and of *Arabidopsis* and tobacco to *M. persicae* increased upon the infection by the non-persistently transmitted cucumber mosaic virus (CMV) due to elevated levels of VOCs released in the air. However, after the initial probing phase in epidermal tissues, virus-infected plants produce antifeedants to discourage aphids from feeding (De Vos *et al.* 2010; Mauck *et al.* 2012; Groen *et al.* 2016). This condition favours the spreading of non-persistently transmitted viruses as the vector leaves the infected host soon after the probing phase during which it did not feed but already acquired virus particles from plant epidermal cells (Hull 2014). Another study was reported in melon plants infected by the non-persistently transmitted watermelon mosaic virus (WMV), family *Potyviridae*, genus *Potyvirus*. Infected plants emit volatiles that induce gene deregulation in neighbouring healthy plants showing significant over-emission of benzaldehyde and  $\gamma$ -butyrolactone. The perception of a volatile signal encoded by WMV-infected tissues triggered a response to prepare healthy tissues of the same plant or/and healthy neighbouring plants for the incoming infections (López-Berenguer *et al.* 2021).

Compared to other plant stressors, virus infections have received minor attention as stimulators of VOCs emissions. In this study, we considered infections of a recombinant strain of potato virus Y (PVY<sup>C-to</sup>), necrogenic to tomato, found in Apulia (southern Italy). PVY, genus *Potyvirus*, family *Potyviridae* (Wylie *et al.* 2017), is a positive-sense, single-stranded RNA virus non-persistently transmitted by several species of aphids to a broad range of plants belonging to 23 different families of dicotyledonous species, including cucurbits, solanaceous and legumes (Gadhavé *et al.* 2020). PVY is one of the most harmful plant viruses because of the severity of disease phenotypes and economic losses caused worldwide (Scholthof *et al.* 2011).

In protected tomato crops, PVY<sup>C-to</sup> infection induced necrotic spots on the upper epidermis of the leaflets that corresponded to translucent necrotic areas on the lower epidermis where some vein necrosis was also visible. Chlorotic/necrotic spots were also scattered on fruit skin. The fully sequenced PVY<sup>C-to</sup> genome

revealed a putative recombination breakpoint in the HC-Pro/P3 coding region and the biological and genome characteristics supported the hypothesis that PVY<sup>C-to</sup> was a recombinant isolate of the isolates belonging to the PVYC2 strain group, which are necrotic on tomato (Mascia *et al.* 2010a). To date, no PVY-resistant tomato varieties are available on the market and no efficient and environmentally friendly methods of control have been described (Scholthof *et al.* 2011).

In tomato, vegetable grafting can attenuate virus disease symptom severity. Grafting onto resistant rootstocks for the control of diseases is widely used in the cultivation of woody trees (Mudge *et al.* 2009) and recently it was extended to vegetable crops such as tomato, eggplant, sweet pepper, watermelon, melon, and cucumber, in Asia, Europe, and North America (Gaion *et al.* 2018). Spanò *et al.* (2020a) showed that tolerance rather than resistance is involved in the resilience to appearance of symptoms and yield losses in grafted tomato plants to manage infections of an Sw5 resistance-breaking strain of tomato spotted wilt virus (TSWV), a CMV strain with necrogenic or stunting satellite RNAs and the tomato necrogenic PVY<sup>C-to</sup> recombinant isolate. Grafted plants showed low accumulation of viral RNA and recovery from disease symptoms, which is a graft-induced tolerant state (Kørner *et al.* 2018). Compared to non-grafted plants, grafted plants employ higher energy resources to respond to graft wounding rather than to infection. For example, mechanical graft wounding alters about 8% of the total genes annotated in *Arabidopsis thaliana* with a high degree of overlapping among genes responsive to wound, abiotic stress and pathogen attack (Spanò *et al.* 2020b). Thus, a combined contribution of the graft, disease symptoms and viral load to the composition of VOCs emissions in virus-infected plants could be expected.

In this study, a headspace solid-phase microextraction-gas chromatography-mass spectrometry (HS-SPME/GC-MS) method was applied to monitor the VOCs emitted by grafted and non-grafted infected tomato plants in relation to PVY<sup>C-to</sup> RNA accumulation in infected tissues and appearance of the disease symptoms and compared to that of mock-inoculated grafted tomato plants. The main objective was to provide new knowledge on the effects of potyvirus necrotic infections on volatillome emitted by a non-model plant species such as tomato. Results were also correlated with the recent data of the tomato transcriptome profile from grafted UC/Ma and non-grafted UC tomato plants upon PVY<sup>C-to</sup> infection and viral RNA accumulation (Spanò *et al.* 2020b), providing evidence of a correlation between volatillome, PVY<sup>C-to</sup> pathogenesis and plant defense response.

## 2. Materials and methods

### 2.1. Chemicals and reagents for HS-SPME/GC-MS

The sodium phosphate dibasic ( $\text{Na}_2\text{HPO}_4$ ,  $\geq 99.0\%$ ), potassium phosphate monobasic ( $\text{KH}_2\text{PO}_4$ ,  $\geq 99.0\%$ ), sodium hydroxide ( $\text{NaOH}$ ,  $\geq 99.0\%$ ), ethylenediaminetetraacetic acid (EDTA,  $\geq 98.5\%$ ), and methanol (HPLC grade) were purchased from Sigma–Aldrich (Milan, Italy). A total of 10 mL headspace vials with crimp cap composed by a pierceable silicon/PTFE septa and Ultra Inert liner Straight (0.75 mm, *i.d.*) were purchased from Agilent Technologies (Palo Alto, CA, USA). Chemical standards (Nonanoic acid, 1-Penten-3-ol, 1-Pentanol, 1-Hexanol, (Z)-3-Hexen-1-ol, (E)-2-Hexen-1-ol, 1-Octen-3-ol, 2-ethyl-1-Hexanol, 1-Octanol, 2-phenyl-Ethanol, Hexanal, (E)-2-Hexenal, Decanal, Benzaldehyde, Methyl ethanoate, Methyl 2-methylbutanoate, Methyl hexanoate, Methyl hexadecanoate, Eugenol, 2-pentyl-Furan, 6-methyl-5-Hepten-2-one,  $\alpha$ -Pinene,  $\alpha$ -Phellandrene,  $\alpha$ -Terpinene, R-Limonene,  $\gamma$ -Terpinene, Terpinolene, Linalool, Caryophyllene, Humulene, and E-Nerolidol) were purchased from Ultra Scientific Italia s.r.l. (Bologna, Italy). Helium at a purity of 99.9995% was obtained by Sapio s.r.l. (Bari, Italy). The manual solid-phase microextraction (SPME) sampler holder and divinylbenzene/carboxen/polydimethylsiloxane (DVB/CAR/PDMS, 50/30  $\mu\text{m}$  film thickness, 1 cm fiber length) fibers were purchased from Supelco (Bellafonte, PA, USA). The 2-methyl-Pentanal ( $\geq 98\%$ ) was obtained from Aldrich Chemical Co. (Milwaukee, WI, USA). A mixture of normal alkanes (C5-C29) was purchased from o2si smart solutions (Charleston, SC, USA).

### 2.2. Plant and virus

*Solanum lycopersicum* plants cv. UC82 (UC) and ecotype Manduria (Ma) were grown under glasshouse condition at 24°C with a 16 h/8 h (light/dark) photoperiod. The susceptible UC tomato variety was used as scion for grafting onto the tolerant Ma tomato ecotype to prepare the UC/Ma grafted plants, as previously described (Spanò *et al.* 2015).

UC and UC/Ma plants were mechanically inoculated by rubbing leaves with sap obtained from leaf tissues of systemically PVY<sup>C</sup>-to-infected UC tomatoes grounded in 100 mmol L<sup>-1</sup> ( $\text{Na}_2\text{-K}$ ) phosphate buffer, pH 7.2.

Grafted plants were inoculated 10 days after grafting on the first leaf above the graft junction, whereas UC/Ma plants inoculated with phosphate buffer served as controls. All the plants were monitored daily for disease symptoms appearance. Six biological replicates were

used for each condition (grafted or non-grafted) and treatment (mock or infected).

### 2.3. Dot-blot analysis

For dot-blot analysis, total RNA was extracted from the second true leaf of tomato plants challenged with PVY<sup>C</sup>-to or mock-inoculated at 28 days post-inoculation (dpi) using TRIzol Reagent (Invitrogen, USA) following manufacturer protocol. Total RNA preparations were subjected to quantitative dot-blot analysis (qDot-blot) using 1  $\mu\text{g}$   $\mu\text{L}^{-1}$  of RNA extract diluted with 6  $\mu\text{L}$  (v/v) of 50 mmol L<sup>-1</sup> NaOH–2.5 mmol L<sup>-1</sup> EDTA and spotted as 10  $\mu\text{L}$  aliquots onto a nylon membrane charged positively (Roche Diagnostics, Mannheim, Germany). Membranes were exposed for 5 min to UV light to cross-link nucleic acids and hybridised overnight at 50°C in 150  $\mu\text{L}$  cm<sup>-2</sup> of DIG Easy Hyb Granules solution (Roche Diagnostics, Mannheim, Germany) containing 50 ng mL<sup>-1</sup> of DIG-labeled DNA probe derived from the coat protein coding region of PVY genome. After hybridisation, probe excess was removed and DIG-chemiluminescent hybrids detected as previously described (Minutillo *et al.* 2012). Chemiluminescent hybridisation signal was detected and quantified by the ChemiDoc system apparatus and Image Lab Software (Bio-Rad Laboratories). Glyceraldehyde 3-phosphate dehydrogenase (GAPDH) was used as housekeeping gene for normalization (Mascia *et al.* 2010b; Spanò *et al.* 2015).

### 2.4. HS-SPME extraction and GC-MS analysis of volatile organic compounds

The VOCs analysis of mock-inoculated and virus-infected tomato leaves collected at 28 dpi at the 3–4 leaf stage was carried out by a HS-SPME/GC-MS method. Specifically, the analysis was carried out by a 6890 Series GC System (Agilent Technologies, Palo Alto, CA, USA) coupled with an Agilent 59753 inert MSD Mass Spectrometer, a MPS 2 Autosampler (Gerstel, Mulheim an der Ruhr, Germany), and using a VF-WAXms (60 m $\times$ 0.25 mm *i.d.*, 0.25- $\mu\text{m}$  film thickness, Agilent Technologies) fused-silica capillary column. In detail, about 150 mg of tomato leaves were collected, placed in a 10 mL headspace vial within 2 min, and kept at temperature of 40°C for 10 min in a water bath. The extraction from the headspace was performed exposing a divinylbenzene/carboxen/polydimethylsiloxane (DVB/CAR/PDMS, 1 cm fiber length) fiber at 40°C for 30 min. After extraction, compounds were thermally desorbed in the split/splitless injector port (Agilent Technologies) of the GC System at 250°C for 5 min. The injection port fitted with a 0.75-mm

*i.d.* Ultra Inert liner Straight was maintained at 250°C in splitless mode. The analyses were performed with the following programmed temperature mode: after 5 min incubation at 40°C, temperature was raised to 140°C at the rate of 2°C min<sup>-1</sup>, to 210°C at the rate of 5°C min<sup>-1</sup>, to 230°C at the rate of 20°C min<sup>-1</sup> and held for 10 min at this final temperature. The total chromatographic run time was 80 min. Each sample was analyzed in triplicate. The helium flow rate was held constant at 1 mL min<sup>-1</sup>. The transfer line, ion source and quadrupole temperatures were 280, 230 and 150°C, respectively. Electron impact ionization (EI+) mode with an electron energy of 70 eV was used. The mass spectrometer acquired data in full scan mode (scan range: 40–300 m/z). The compounds were identified by comparison of experimental mass spectra with spectra in the NIST/EPA/NIH Mass Spectral Database (National Institute of Standards and Technology, version 2.0 f, USA) using a match quality higher than 80. The identification of volatile compounds was also verified by comparison their linear retention indices (LRI), determined as Kovats indices, in relation to the retention times of C5–C29 n-alkanes series and compared with those reported in literature (Zellner *et al.* 2008; [www.chemspider.com](http://www.chemspider.com); [www.flavornet.org/f\\_kovats.html](http://www.flavornet.org/f_kovats.html); [www.nist.gov](http://www.nist.gov); [www.pherobase.com](http://www.pherobase.com)). Quantification of compounds was performed with internal standardization by adding 2.5 µL of 500 mg L<sup>-1</sup> 2-methyl-Pentanal. The quantitative evaluation of the compounds was determined as ratio between their peak areas and the 2-methyl-Pentanal peak area.

## 2.5. RNAseq analysis

For RNAseq experiments, total RNA samples were prepared from non-grafted UC and UC/Ma grafted plants infected by PVY<sup>C</sup>-to in three biological replicates at 14 dpi, before the appearance of the recovery phenotype. Total RNA was extracted using EuroGOLD RNAPure™ (EuroClone) according to Spanò *et al.* (2020b). Quantity and quality of RNA were estimated by Qubit RNA HS Assay Kit (ThermoFisher Scientific, USA) and Bioanalyzer 1000 (Agilent Technologies, Santa Clara, USA). Samples with RNA integrity number (RIN) ≥ 7 were used for selective ribosomal depletion using RiboMinus™ Eukaryote System v2 (ThermoFisher Scientific) and complementary DNA libraries preparation using Ion Total RNA-Seq Kit v2 according to Spanò *et al.* (2020b). A total of 100 pmol L<sup>-1</sup> of each cDNA libraries were sequenced on an Ion S5 System using an Ion 540-OT2 Kit (ThermoFisher Scientific) following manufacturer's instructions and pre-processed using the Ion Torrent Suite™ Software (Ion Torrent, ThermoFisher Scientific) according to Spanò

*et al.* (2020b). Quality filtered sequenced reads were analyzed using Galaxy platform and aligned against *Solanum lycopersicum* annotated genome sequence (ENSEMBL SL2.50\_37 version) using HISAT2 Spliced Alignment Program (Langmead *et al.* 2009; Kim *et al.* 2015). Differentially expressed genes (DEGs) with a fold change (FC) expression values of absolute logarithm (to basis 2) greater or equal to one ( $|\log_2 FC| \geq 1$ ) for  $P \leq 0.05$  were selected using the DESeq2 (Anders *et al.* 2010) between PVY<sup>C</sup>-to-infected grafted and non-grafted plants.

## 2.6. Statistical analysis

Statistical analyses of the peak area ratios of the detected compounds were done by comparing two independent samples applying a nonparametric test (Mann–Whitney U test, with  $P \leq 0.05$ ), using the software system STATISTICA (StatSoft.Inc. v.7, 2004). For principal component analysis (PCA) of the volatile profile, the HS-SPME/GC-MS data were processed by the multivariate data analysis software chemometrics agile tool (CAT), freely accessible by <http://www.gruppochemiometria.it/index.php/software>.

## 3. Results

### 3.1. PVY<sup>C</sup>-to-infected tomato plants displayed symptoms correlated with viral RNA accumulation

All the non-grafted UC plants inoculated with PVY<sup>C</sup>-to were systemically infected showing by 28 dpi generalized suffering, leaf blade reduction, thickening and twisting with necrotic areas at the leaf blade tips, visible on the upper and lower side and showed the expected disease phenotype of PVY<sup>C</sup>-to infection.

On the contrary, PVY<sup>C</sup>-to infection in UC/Ma grafted plants caused mild distortion and reduction of the young leaves. These symptoms disappeared as the leaf blade expanded (Fig. 1).

Viral RNA accumulation in leaf samples from 6 biological replicates was approx 4-fold higher in UC than in UC/Ma (Table 1). All UC/Ma-grafted plants recovered from disease symptoms between 21 and 28 dpi, but no UC plants that showed increasing disease severity until 30 dpi when symptom monitoring was terminated. According to previous results (Spanò *et al.* 2020b), both the graft and the Ma genotype used as rootstock contributed to reduce viral RNA accumulation in the scion allowing the grafted plants to recover from disease symptoms.





**Fig. 1** Generalized suffering, leaf blade reduction, thickening and twisting with some necrosis at tips of leaf blade shown by non-grafted UC82 (UC) at 28 days post-inoculation (dpi) with the recombinant strain of potato virus Y (PVY<sup>C-to</sup>) (A), compared to milder symptoms shown by UC82 (UC) plants grafted onto Manduria (UC/Ma) plants, which substantially recovered from disease symptoms between 21 and 28 dpi (C). Mock-inoculated controls of grafted UC/Ma are in B.

**Table 1** Quantitative estimation of the recombinant strain of potato virus Y (PVY<sup>C-to</sup>) RNA accumulation (ng/μg leaf tissue) in non-grafted UC82 (UC) and in UC82 plants grafted onto Manduria (UC/Ma) at 28 days post-inoculation (dpi)

Plant <sup>1)</sup>	Symptoms <sup>2)</sup>	Viral RNA titre <sup>3)</sup>
UC	LD, N	0.2±0.02
UC/Ma	mLD, R	0.05±0.015

<sup>1)</sup> UC/Ma=Scion/Rootstock.

<sup>2)</sup> LD, N=leaf distortion and tip leaf necrosis; mLD, R=mild leaf distortion and recovery.

<sup>3)</sup> Data are pg of viral RNA estimated by quantitative dot-blot hybridization at 28 dpi. Each value represents average of six biological replicates±standard error among replicates.

### 3.2. Disease symptoms altered differentially the VOCs bouquet of PVY<sup>C-to</sup>-infected tomato leaves

Biotic stress can induce changes in the composition of plant VOCs blend that are qualitatively and quantitatively unique. Moreover, different plant organs emit diverse VOCs profile under stress (Gargallo-Garriga *et al.* 2014). To examine the VOCs involved in the tomato–PVY<sup>C-to</sup> interaction, tomato volatilome was analyzed in UC+PVY<sup>C-to</sup>, UC/Ma+PVY<sup>C-to</sup> and UC/Ma mock-inoculated plants by

HS-SPME/GC-MS analysis at 28 dpi and after 38 days from the graft wound, when it was well sealed and the recovery process in grafted plants was completed. According to Kumar (2018), complete sealing of graft wound would be achieved between 7 and 10 days after grafting. Thus, in this analysis we were confident that significant influence on the VOCs emission derived from virus infection rather than from unsealed graft wound.

As reported in Table 2, the HS-SPME/GC-MS analysis detected a total of 111 VOCs: 41 terpenes, 19 alcohols, 14 esters, 6 aldehydes, 4 ketones, 4 ethers, 2 heterocycles, 1 acid, 1 hydrocarbon, and 19 unknown compounds. All compounds were quantified except 4 due to inadequate chromatographic resolution. Non-quantifiable compounds were excluded in the subsequent data evaluations.

Venn diagram of the volatilome emerged from the gas chromatogram and characterized by mass spectrometry revealed 98 VOCs shared among UC+PVY<sup>C-to</sup>, UC/Ma+PVY<sup>C-to</sup> and UC/Ma mock plants (Fig. 2) and six compounds shared between non-grafted UC plants and UC/Ma plants infected by PVY<sup>C-to</sup>, namely 2-pentyl-Furan, *trans*-β-Ocimene, 4-Hexen-1-ol, *o*-Guaiacol, E-Nerolidol

**Table 2** List of the total volatile organic compounds (VOCs) identified in tomato leaves by headspace solid-phase microextraction-gas chromatography-mass spectrometry (HS-SPME/GC-MS) analysis

Volatile compound	LRI <sub>lit</sub> /LRI <sub>sp</sub> <sup>1)</sup>	Volatile compound	LRI <sub>lit</sub> /LRI <sub>sp</sub> <sup>1)</sup>
Acids		2-Carene; 4-Carene <sup>3)</sup>	1 131; 1 128/1 131
Nonanoic acid <sup>2)</sup>	2 166/2 166	2-Carene; 4-Carene <sup>3)</sup>	1 137; 1 144/1 137
Alcohols		α-Phellandrene <sup>2)</sup>	1 165/1 165
3-Pentanol	1 120/1 120	α-Terpinene <sup>2)</sup>	1 180/1 180
1-Penten-3-ol <sup>2)</sup>	1 169/1 169	Terpene <sup>1 4)</sup>	–/1 185
1-Pentanol <sup>2)</sup>	1 258/1 258	R-Limonene <sup>2)</sup>	1 201/1 201
2-methyl-1-Pentanol	1 312/1 308	β-Phellandrene	1 212/1 212
(Z)-2-Penten-1-ol	1 329/1 329	<i>cis</i> -β-Ocimene	1 239/1 239

(Continued on next page)

**Table 2** (Continued from preceding page)

Volatile compound	LRI <sub>l</sub> /LRI <sub>sp</sub> <sup>1)</sup>	Volatile compound	LRI <sub>l</sub> /LRI <sub>sp</sub> <sup>1)</sup>
3-methyl-1-Pentanol	1334/1334	γ-Terpinene <sup>2)</sup>	1248/1248
1-Hexanol <sup>2)</sup>	1362/1362	trans-β-Ocimene	1256/1256
(E)-3-Hexen-1-ol	1371/1371	Cymene	1273/1273
(Z)-3-Hexen-1-ol <sup>2)</sup>	1395/1395	Terpinolene <sup>2)</sup>	1285/1285
(E)-2-Hexen-1-ol <sup>2)</sup>	1414/1414	p-Cymenene	1444/1444
(E)-4-Hexen-1-ol; (Z)-4-Hexen-1-ol <sup>3)</sup>	1413; 1422/1420	α-Cubebene	1460/1460
(E)-4-Hexen-1-ol; (Z)-4-Hexen-1-ol <sup>3)</sup>	1413; 1422/1435	Terpene 2 <sup>4)</sup>	-/1468
1-Octen-3-ol <sup>2)</sup>	1457/1457	δ-Elementene	1473/1473
1-Heptanol	1463/1463	α-Copaene	1493/1493
2-ethyl-1-Hexanol <sup>2)</sup>	1496/1496	Linalool <sup>2)</sup>	1555/1555
1-Octanol <sup>2)</sup>	1566/1566	β-Elementene	1595/1595
Benzyl alcohol	1890/1890	Caryophyllene <sup>2)</sup>	1602/1602
2-phenyl-Ethanol	1923/1923	Terpene 3 <sup>4)</sup>	-/1608
Phenol	2002/2002	Terpene 4 <sup>4)</sup>	-/1615
Aldehydes		Terpene 5 <sup>4)</sup>	-/1620
Hexanal <sup>2)</sup>	1091/1091	Terpene 6 <sup>4)</sup>	-/1632
3-Hexenal	1149/1152	γ-Elementene	1641/1640
(E)-2-Hexenal <sup>2)</sup>	1226/1226	Terpene 7 <sup>4)</sup>	-/1665
(E,E)-2,4-Hexadienal	1411/1410	Humulene <sup>2)</sup>	1670/1670
Decanal <sup>2)</sup>	1507/1507	Terpene 8 <sup>4)</sup>	-/1673
Benzaldehyde <sup>2)</sup>	1533/1533	Terpene 9 <sup>4)</sup>	-/1687
Esters		Terpene 10 <sup>4)</sup>	-/1691
Methyl ethanoate <sup>2)</sup>	864/866	Terpene 11 <sup>4)</sup>	-/1707
Methyl 2-methylbutanoate <sup>2)</sup>	1022/1021	Terpene 12 <sup>4)</sup>	-/1718
Methyl 3-methylbutanoate	1025/1029	Terpene 13 <sup>4)</sup>	-/1725
Methyl hexanoate <sup>2)</sup>	1194/1194	Terpene 14 <sup>4)</sup>	-/1740
Methyl 3-hexenoate	1260/1266	Terpene 15 <sup>4)</sup>	-/1762
Methyl (E)-2-hexenoate	1305/1297	3,7(11)-Selinadiene	1778/1782
4-Hexen-1-yl acetate; 3-Hexen-1-yl acetate <sup>3)</sup>	1326; 1315/1324	Terpene 16 <sup>4)</sup>	-/1830
Methyl nonanoate	1500/1498	Terpene 17 <sup>4)</sup>	-/1834
Methyl decanoate	1600/1600	Caryophyllene oxide	1984/1984
Methyl benzoate	1628/1629	E-Nerolidol <sup>2)</sup>	2033/2032
Methyl salicylate	1785/1785	Unknown <sup>5)</sup>	
Methyl dodecanoate	1808/1808	Unknown 1	-/982
Methyl tetradecanoate	2000/2000	Unknown 2	-/1177
Methyl hexadecanoate <sup>2)</sup>	2207/2207	Unknown 3	-/1321
Ethers		Unknown 4	-/1542
1-butoxy-2-Propanol	1343/1346	Unknown 5	-/1561
1,3-dimethoxy-Benzene	1761/1759	Unknown 6	-/1577
o-Guaiacol	1875/1875	Unknown 7	-/1580
Eugenol <sup>2)</sup>	2173/2173	Unknown 8	-/1648
Heterocycles		Unknown 9	-/1715
2-ethyl-Furan	965/968	Unknown 10	-/1721
2-pentyl-Furan <sup>2)</sup>	1236/1236	Unknown 11	-/1771
Hydrocarbons		Unknown 12	-/1813
Undecane	1100/1099	Unknown 13	-/1973
Ketones		Unknown 14	-/2018
3-Pentanone	997/994	Unknown 15	-/2253
6-methyl-5-Hepten-2-one <sup>2)</sup>	1344/1344	Unknown 16	-/2299
β-Ionone	1947/1946	Unknown 17	-/2338
6,10,14-trimethyl-2-Pentadecanone	2125/2125	Unknown 18	-/2382
Terpenes		Unknown 19	-/2430
α-Pinene <sup>2)</sup>	1027/1027		

<sup>1)</sup> LRI<sub>l</sub>, linear retention indices reported in literature by www.nist.gov; LRI<sub>sp</sub>, linear retention indices calculated against n-alkanes (C5–C29) on VF-WAXms column.

<sup>2)</sup> Volatile compounds identified with chemical standard.

<sup>3)</sup> Pair of volatile compounds with similar structure and LRI which cannot exactly identify.

<sup>4)</sup> Unidentified terpenes.

<sup>5)</sup> Unidentified volatile compounds.

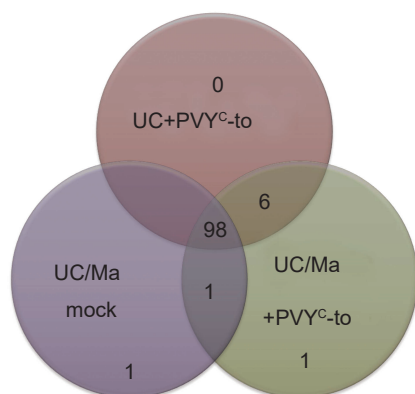


**Fig. 2** The recombinant strain of potato virus Y (PVY<sup>c-to</sup>) infection quantitatively alters the blend of volatile organic compounds (VOCs) emitted by tomato plants. VOCs were collected by headspace trapping from UC82 (UC) plants grafted onto Manduria (UC/Ma) mock-inoculated (mock) or UC and UC/Ma infected by PVY<sup>c-to</sup>. Venn diagram shows the number of common and uncommon VOCs emitted comparing the three biological conditions tested UC+PVY<sup>c-to</sup>, UC/Ma+PVY<sup>c-to</sup> and UC/Ma mock plants.

and one unknown compound.

Methyl tetradecanoate could be attributed to the Ma rootstock as it was shared only by grafted tomato plants, either infected or mock-inoculated, whereas 1-butoxy-2-Propanol was detected only in mock-inoculated UC/Ma plants and could be attributed to Ma rootstock as well. Finally, grafted tomatoes infected by PVY<sup>c-to</sup> specifically emitted *cis*- $\beta$ -Ocimene. Total VOC emissions were 100 for UC/Ma mock-inoculated plants and 106 and 104 for UC/Ma and UC infected by PVY<sup>c-to</sup>, respectively.

To get a general overview of the variations in the volatilome following PVY<sup>c-to</sup> infection in UC tomato plants grafted or not on Ma, a principal component analysis (PCA) was performed on all HS-SPME/GC-MS data. As shown in Fig. 3, by plotting the scores of the samples in the sub-space PC1 vs. PC2 (accounting for 57.2 and 12.0% of the total variance, respectively) a separation between the UC samples infected by PVY<sup>c-to</sup> and those of UC/Ma (infected or not with PVY<sup>c-to</sup>) was observed, suggesting that volatilome of grafted infected tomato leaves was much closer to that of mock-inoculated grafted plants than to that of infected non-grafted UC. The separation observed in this PCA score plot indicated that the VOCs profile was related to accumulation of viral RNA and disease phenotype rather than to the grafted or non-grafted condition. These results supported the assumption of considering the graft wound completely sealed at 28 dpi and therefore not influencing the VOCs profile at that time-point.

To provide information about which variable VOC was more important in calculating the PCs and therefore

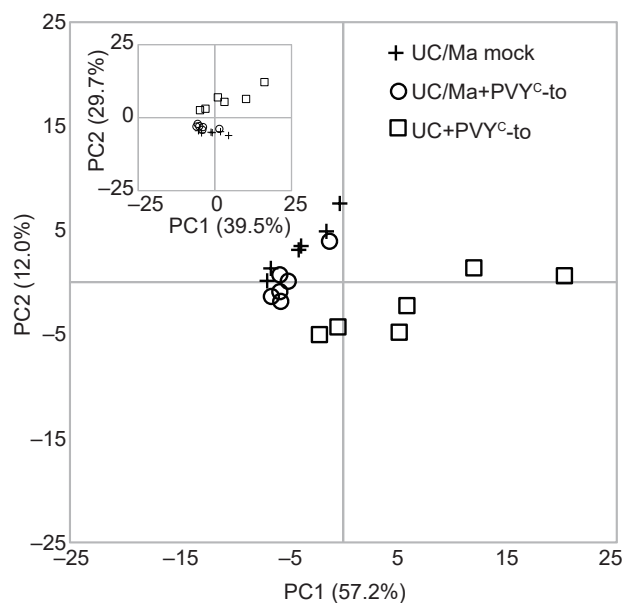


**Fig. 3** Score plots of headspace solid-phase microextraction-gas chromatography-mass spectrometry (HS-SPME/GC-MS) data for leaf samples of UC82 (UC) plants grafted onto Manduria (UC/Ma) mock-inoculated, UC/Ma infected with the recombinant strain of potato virus Y (UC/Ma+PVY<sup>c-to</sup>) and UC+PVY<sup>c-to</sup> at 28 days post-inoculation (dpi) before and after Varimax rotation (inset).

mostly responsible of the resulting separation observed in the Fig. 3, loading values can be used. In fact, the loadings are from a numerical point of view, equal to the coefficients of the variables, and provide information about which VOCs give the largest contribution to the components. High absolute loading indicate that a particular VOC has a strong relationship to a particular principal component. Positive loading indicate that a VOC and a principal component are positively correlated whereas negative loading indicate a negative correlation. A coefficient threshold absolute value must be decided to deem the variable under consideration as important: Specialized knowledge or an arbitrary cut-off value can be used for this purpose.

Moreover, to simplify the interpretation of the results, a rotation of PCs is often adopted such as Varimax rotation, which maximizes the sum of the variance of the squared loadings. This rotation usually results in high loadings for a smaller number of variables and low loadings for the rest. In simple terms, the result is a small number of highlighted important variables, which makes it easier to interpret results. Herein, after a Varimax rotation, the VOCs mainly related to the sample clusterization, i.e., UC+PVY<sup>c-to</sup> samples vs. UC/Ma+PVY<sup>c-to</sup> and UC/Ma mock-inoculated ones, were those with higher absolute loading values on rotated component 2 (see inset of Fig. 3). In addition, only VOCs with an absolute loading

greater than 0.1 (an arbitrary cut-off value that led to not taking into account VOCs with loading smaller than or equal to the 50% of the largest absolute loading value) were considered to characterize the cluster pattern and were reported hereafter.

VOCs with positive loading values, i.e., 11 alcohols [4-Hexen-1-ol, (E)-3-Hexen-1-ol, (E)-2-Hexen-1-ol, 2-ethyl-1-Hexanol, 4-Hexen-1-ol, Benzyl alcohol, (Z)-2-Penten-1-ol, 1-Hexanol, 1-Heptanol, (Z)-3-Hexen-1-ol, 1-Octanol], 5 aldehydes [(E,E)-2,4-Hexadienal, Benzaldehyde, (E)-2-Hexenal, Hexanal, 3-Hexenal], 4 esters [(Hexen-1-yl acetate, Methyl nonanoate, Methyl salicylate, Methyl (E)-2-hexenoate]; 2 heterocycles (2-ethyl-Furan, 2-pentyl-Furan), 2 Ketones (3-Pentanone, 6-methyl-5-Hepten-2-one), 4 unknown compounds (Unknown 4, Unknown 9, Unknown 13, Unknown 11), 1 ether (o-Guaiacol), and 1 terpene (Linalool), corresponded to compounds whose emissions increased with increasing PVY<sup>C</sup>-to RNA accumulation and disease symptoms. On the contrary, the emissions of VOCs with negative loading values, i.e., 2 esters (1-butoxy-2-Propanol, Methyl 3-methylbutanoate), 2 terpenes (Terpene 11 e 17), and 1 ether (1,3-dimethoxy-Benzene), decreased for higher RNA virus accumulation and increased intensity of disease symptoms.

### 3.3. Correlation of the VOCs profiles of tomato leaves upon infection with PVY<sup>C</sup>-to unravelled specific volatile emissions associated with viral RNA accumulation and tomato transcriptome

To identify VOCs associated with the symptomatology/disease phenotype observed, UC and UC/Ma plants infected by PVY<sup>C</sup>-to were statistically analyzed (U-test using  $P \leq 0.05$ ) evidencing 53 volatiles over-emitted upon viral RNA accumulation and disease symptoms appearance (Table 3). Comparison of the VOCs profile between mock and infected UC/Ma plants allowed the identification of 34 statistically differentially emitted VOCs (DVOCs) (Table 4).

Venn diagram (Fig. 4-A) shows that

**Table 3** List of the differentially induced volatile organic compounds (DVOCs) in tomato leaves upon infection of the recombinant strain of potato virus Y (PVY<sup>C</sup>-to) in susceptible UC82 plants (UC) and tolerant UC plants grafted onto Manduria (UC/Ma) at 28 days post-inoculation (dpi)

Volatile compound	UC+PVY <sup>C</sup> -to	UC/Ma+PVY <sup>C</sup> -to	P-value of
			UC+PVY <sup>C</sup> -to vs. UC/Ma+PVY <sup>C</sup> -to <sup>1)</sup>
Methyl ethanoate	3.350±0.384	0.604±0.061	0.006*
2-ethyl-Furan	1.160±0.212	0.205±0.039	0.006*
Unknown 1	0.573±0.060	0.251±0.057	0.006*
3-Pentanone	0.737±0.159	0.142±0.018	0.006*
Undecane	1.437±0.178	0.678±0.136	0.013
3-Pentanol	0.232±0.106	0.036±0.027	0.049
3-Hexenal	0.438±0.109	0.181±0.050	0.044
1-Penten-3-ol	1.010±0.393	0.346±0.047	0.044
α-Terpinene	7.050±2.234	2.360±0.306	0.017
Methyl hexanoate	0.757±0.192	0.172±0.031	0.006*
(E)-2-Hexenal	10.067±1.957	2.082±0.526	0.010
2-pentyl-Furan	0.141±0.038	0.017±0.011	0.005*
1-Pentanol	0.448±0.044	0.168±0.021	0.006*
Methyl 3-hexenoate	4.217±0.598	1.204±0.264	0.006*
Cymene	6.017±1.760	2.420±0.263	0.027
Methyl (E)-2-hexenoate	0.280±0.060	0.092±0.014	0.006*
2-methyl-1-Pentanol	40.500±5.038	15.340±3.404	0.006*
Unknown 3	0.362±0.043	0.106±0.017	0.006*
4-Hexen-1-yl acetate;	0.280±0.052	0.020±0.012	0.005*
3-Hexen-1-yl acetate			
(Z)-2-Penten-1-ol	2.050±0.304	0.596±0.113	0.006*
6-methyl-5-Hepten-2-one	0.174±0.034	0.039±0.017	0.005*
1-Hexanol	29.333±4.951	6.880±0.756	0.006*
(E)-3-Hexen-1-ol	4.083±0.264	1.000±0.112	0.005*
(Z)-3-Hexen-1-ol	208.333±26.130	57.800±9.759	0.006*
(E,E)-2,4-Hexadienal	1.500±0.093	0.260±0.042	0.006*
(E)-2-Hexen-1-ol	11.083±1.624	2.200±0.324	0.006*
(E)-4-Hexen-1-ol	0.670±0.085	0.081±0.032	0.006*
(Z)-4-Hexen-1-ol	0.233±0.022	0.036±0.013	0.006*
p-Cymenene	0.329±0.099	0.088±0.019	0.035
1-Heptanol	0.758±0.073	0.176±0.033	0.006*
α-Copaene	0.253±0.041	0.076±0.015	0.010
2-ethyl-1-Hexanol	13.767±1.839	5.420±1.618	0.017
Methyl nonanoate	2.183±0.336	0.281±0.124	0.006*
Unknown 4	0.183±0.030	0.006±0.006	0.005*
Linalool	0.928±0.373	0.041±0.019	0.006*
Unknown 5	0.310±0.054	0.121±0.022	0.017
1-Octanol	0.498±0.049	0.056±0.019	0.006*
Unknown 6	2.227±0.426	1.010±0.173	0.044
Unknown 7	0.597±0.090	0.232±0.035	0.010
Terpene 4	4.800±0.874	2.040±0.388	0.044
Unknown 8	2.967±0.514	1.090±0.199	0.017
Terpene 8	1.625±0.377	0.660±0.162	0.028
Terpene 9	0.623±0.125	0.183±0.035	0.006*
Unknown 9	2.333±0.466	0.319±0.083	0.006*
Unknown 11	0.388±0.048	0.128±0.018	0.005*
Methyl salicylate	25.500±6.350	3.200±0.797	0.005*
Methyl dodecanoate	0.267±0.048	0.051±0.019	0.007*
Unknown 12	0.869±0.498	0.033±0.015	0.006*
2-phenyl-Ethanol	1.375±0.165	0.716±0.171	0.035
Unknown 13	1.482±0.209	0.464±0.090	0.010
Methyl hexadecanoate	0.297±0.049	0.123±0.024	0.027
Unknown 17	0.398±0.084	0.141±0.029	0.017
Unknown 19	0.453±0.115	0.074±0.006	0.006*

<sup>1)</sup> Values are expressed as analyte/internal standard peak area ratios upon U-test analyses with  $P \leq 0.05$ .

Values are expressed as mean±standard error of six samples for each group. \*, 33 differentially emitted VOCs for  $P \leq 0.01$  in Mann–Whitney U-test analyses.



**Table 4** List of the differentially induced volatile organic compounds (DVOCs) shared between mock and infected UC82 (UC) plants grafted onto Manduria (UC/Ma) at 28 days post-inoculation (dpi)

Volatile compound	UC/Ma mock	UC/Ma+PVY <sup>C</sup> -to	P-value of UC/Ma mock vs. UC/Ma+PVY <sup>C</sup> -to <sup>1)</sup>
Methyl ethanoate	3.000±0.318	0.604±0.061	0.014
UNKNOWN 1	0.595±0.046	0.250±0.057	0.014
3-Pentanone	0.042±0.024	0.142±0.018	0.013
Methyl 2-methylbutanoate	1.700±0.506	0.284±0.132	0.013
Methyl 3-methylbutanoate	2.550±0.877	0.234±0.072	0.014
Hexanal	0.153±0.020	0.488±0.077	0.014
Undecane	1.525±0.143	0.678±0.136	0.026
3-Hexenal	0.028±0.027	0.181±0.049	0.046
Methyl hexanoate	1.365±0.495	0.172±0.030	0.014
<i>trans</i> -β-Ocimene	0.000±0.000	0.550±0.0512	0.031
1-Pentanol	0.295±0.059	0.168±0.021	0.035
Methyl 3-hexenoate	4.250±0.284	1.204±0.263	0.013
Methyl (E)-2-hexenoate	0.158±0.016	0.092±0.013	0.027
2-methyl-1-Pentanol	53.750±5.437	15.340±3.403	0.014
1-butoxy-2-Propanol	1.595±0.246	0.001±0.000	0.010
(Z)-3-Hexen-1-ol	102.500±4.787	57.800±9.759	0.026
(E,E)-2,4-Hexadienal	0.060±0.034	0.260±0.042	0.013
(E)-4-Hexen-1-ol	0.200±0.024	0.081±0.031	0.024
(Z)-4-Hexen-1-ol	0.000±0.000	0.036±0.012	0.031
1-Heptanol	0.340±0.029	0.176±0.032	0.013
α-Copaene	0.150±0.021	0.076±0.014	0.049
Benzaldehyde	0.153±0.028	0.622±0.104	0.013
1-Octanol	0.333±0.062	0.056±0.018	0.013
Methyl benzoate	0.102±0.008	0.328±0.055	0.014
Terpene 9	0.395±0.058	0.183±0.035	0.027
Methyl dodecanoate	0.400±0.084	0.051±0.018	0.014
o-Guaiacol	0.000±0.000	0.113±0.022	0.010
2-phenyl-Ethanol	1.650±0.287	0.716±0.171	0.026
β-Ionone	0.155±0.021	0.034±0.021	0.012
E-Nerolidol	0.000±0.000	0.052±0.019	0.031
Nonanoic acid	0.823±0.163	0.370±0.096	0.049
Methyl hexadecanoate	0.335±0.054	0.123±0.024	0.014
Unknown 15	0.102±0.041	0.226±0.017	0.019
Unknown 19	0.208±0.048	0.074±0.005	0.014

<sup>1)</sup> Values are expressed as analyte/internal standard peak area ratios upon U-test analyses with  $P \leq 0.05$ . Values are expressed as mean±standard error of six samples for each group.

among the 53 and 34 volatiles emerged from the two comparisons, there were 22 DVOCs shared by the UC+PVY<sup>C</sup>-to, UC/Ma+PVY<sup>C</sup>-to and UC/Ma mock plants. A specific set of 31 DVOCs in infected plants of UC/Ma compared with UC were related to the virus induced symptoms and belonged to heterocycles, alcohols, terpenes, aldehydes, ketones, and esters families (Fig. 4-B). All the 31 DVOCs were over-emitted in symptomatic UC+PVY<sup>C</sup>-to plants, compared to UC/Ma+PVY<sup>C</sup>-to plants (Fig. 4-B). Another set of 12 DVOCs was identified in UC/Ma plants from the comparison between infected and mock-inoculated. Benzaldehyde, Methyl benzoate, Hexanal, *trans*-β-Ocimene stood out for over intensity of emission in grafted tomato plants upon PVY<sup>C</sup>-to infection (Fig. 4-C). These DVOCs are known as volatile compounds closely related to the plant defense

mechanisms (Fig. 4-C).

Finally, 11 unidentified DVOCs were found in the comparison of DVOCs between UC and UC/Ma infected plants as they were not differentially emitted in the DVOCs blends of mock-inoculated grafted tomato plants (Fig. 4-B).

In addition, a striking decrease in the complexity and in the overall quantity of the DVOCs were observed in the comparison between UC/Ma+PVY<sup>C</sup>-to vs. UC/Ma mock (12 DVOCs) and UC/Ma+PVY<sup>C</sup>-to vs. UC+PVY<sup>C</sup>-to (31 DVOCs) (Figs. 3 and 4-B–E).

A more stringent statistical analysis (U-test with  $P \leq 0.01$ ) detected 33 DVOCs between non-grafted UC+PVY<sup>C</sup>-to and UC/Ma+PVY<sup>C</sup>-to plants (Table 3, labeled with \*), whereas no DVOCs were identified between UC/Ma+PVY<sup>C</sup>-to and UC/Ma mock-inoculated, suggesting that

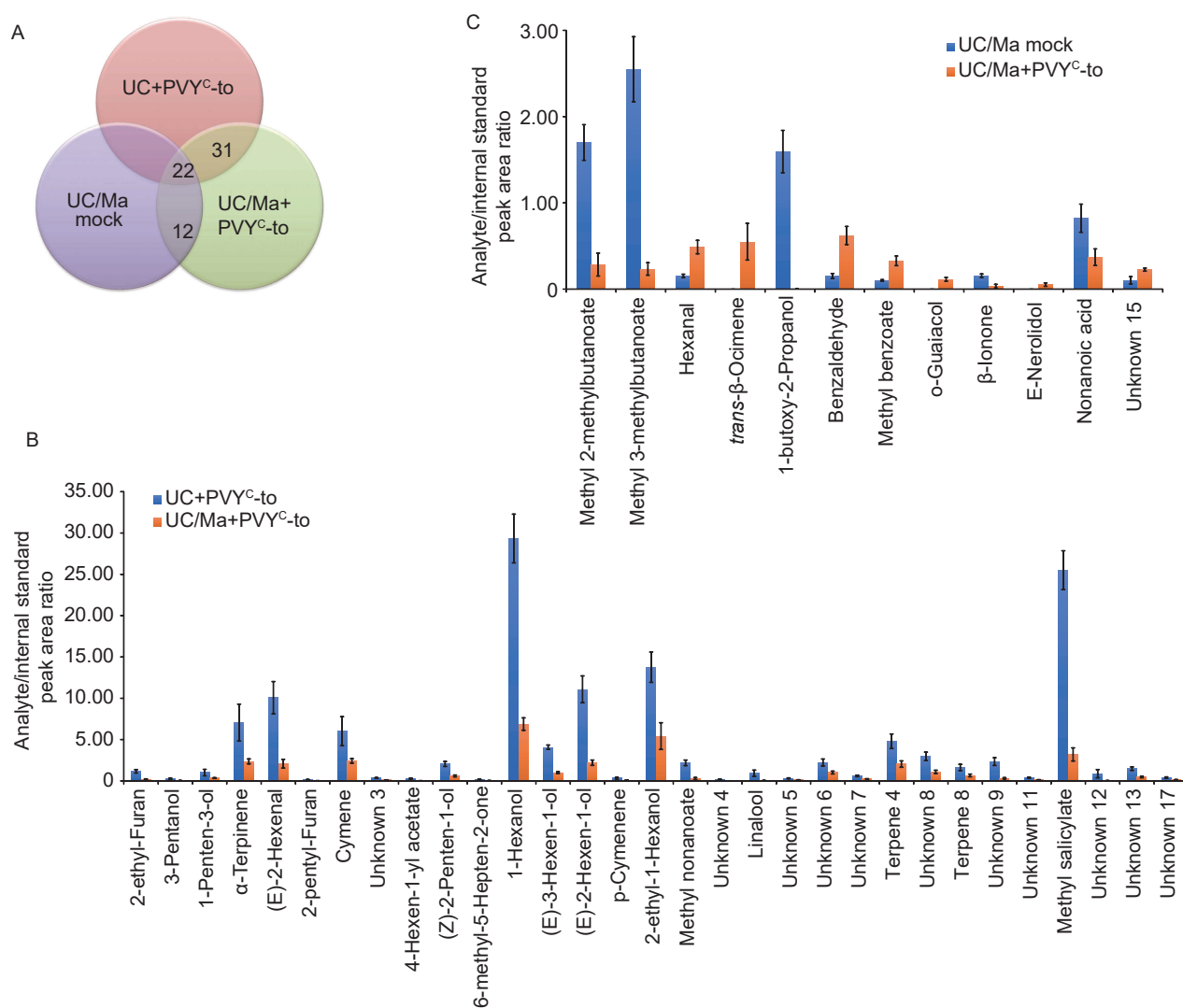


**Fig. 4** Comparison of volatile organic compound (VOC) profiles. A, the Venn diagram shows the number of shared and unshared differentially emitted VOCs comparing UC82 plants infected with the recombinant strain of potato virus Y (UC+PVY<sup>c</sup>-to) vs. infected UC82 (UC) plants grafted onto Manduria (UC/Ma+PVY<sup>c</sup>-to) and UC/Ma mock vs. UC/Ma+PVY<sup>c</sup>-to upon Mann-Whitney U-test analyses with  $P \leq 0.05$ . "Shared" are those differentially emitted VOCs identified in both comparisons and "unshared" are those specific for each comparison. B and C, unique differentially induced VOCs emitted from diseased plants upon PVY<sup>c</sup>-to infection in susceptible UC with high accumulation of virus and tolerant UC/Ma plants (B), and from UC/Ma plants that had been mock or inoculated with PVY<sup>c</sup>-to (C) are shown. The columns represent the mean of analyte/internal standard peak area ratios upon Mann-Whitney U-test analyses with  $P \leq 0.05$ , and error bars represent the variation (standard error,  $n=6$ ).

VOCs emission was strongly induced by the increase of disease symptoms intensity.

In order to correlate the DVOCs outline with the data of the tomato transcriptome profile and, in turn, with virus RNA accumulation in infected plants, total reads were obtained from sequencing cDNA libraries prepared from UC and UC/Ma plants infected by PVY<sup>c</sup>-to. Reads ranged from 19 921 687 to 34 459 114 with a mean reads length of 149 bp and about 88.7% of the total reads mapped to *S. lycopersicum* genome (ENSEMBL SL2.50\_37). cDNA libraries for RNA sequencing were prepared from leaf

samples collected at 14 dpi with PVY<sup>c</sup>-to infection. The 14 dpi time-point corresponded to a situation in which both UC and UC/Ma infected plants showed symptoms, as the recovery from disease symptoms in grafted plants was visible only by 21 dpi. Therefore 14 dpi seemed the most appropriate infection time-point to collect samples for the correlation between VOCs emissions and the identification of DEGs ( $P \leq 0.05$ ). From the 33 810 annotated genes in *S. lycopersicum* genome (Solyc), 1 144 DEGs were obtained, corresponding to approx 3.38% of total Solyc annotated genes. Among these, the

transcriptional activation of tomato pathogenesis-related (PR) protein genes was detected, with statistically different gene expression levels in infected plants of UC/Ma compared with UC, evidencing a positive correlation between the differential expression of these genes and the PVY<sup>C</sup>-to RNA accumulation (Table 5). Furthermore, an up-regulation of *S. lycopersicum salicylic acid carboxyl methyltransferase* gene (*SI-SAMT*) was detected with a fold change (FC) of 2.71 between UC and UC/Ma infected plants (Table 5). This result is congruent with the over-emission of benzenoids in UC leaves compared to the UC/Ma-infected plants, suggesting that the induction of benzenoid derivatives, such as the SA derivatives methyl salicylate (MeSA) could contribute specifically in the plant defense response to virus infection (Table 5). In UC diseased-leaves, we also detected enhanced emissions of volatile molecules such as C5 and C6 aldehydes, alcohols and derivatives [(Z)-3-Hexen-1-ol, 2-Hexen-1-ol, 1-Hexanol, 2-ethyl-1-Hexanol, 2-methyl-1-Pentanol, (Z)-2-Penten-1-ol, 1-Penten-3-ol], generally referred to as green leaf volatiles (GLVs) (Bellés et al. 2008). These compounds are products of the lipoxygenase (LOX) pathway, an important plant fatty acid metabolic pathway (Wei et al. 2013), whose production and release could be associated to the effective plant defense response against virus infection. Indeed, the differential GLVs production detected in the VOCs bouquet of diseased tomato leaves was consistent with the differential transcriptional activation of the *S. lycopersicum TomLoxF* biosynthesis-related gene, with a FC of 1.43 (Table 5) in UC compared to UC/Ma-infected plants, suggesting a possible role of the biosynthesis of GLV esters in tomato defense response against PVY<sup>C</sup>-to infection. As a result of these untargeted metabolomic analyses, we could conclude that PVY<sup>C</sup>-to disease severity in tomato at 14 dpi induced the emission of a volatilome, which, on the whole, appears enriched in susceptible PVY<sup>C</sup>-to-infected UC, compared to tolerant PVY<sup>C</sup>-to-infected UC/Ma plants.

## 4. Discussion

VOCs emitted by vegetation are a heterogeneous set of chemical molecules with a wide range of functions for plants, and consequences for the ecosystem and the environment. Plants attacked by herbivore insects and pathogens, release chemicals into the air that can be detected by healthy neighbouring plants activating signals based on insecticidal or defence compounds to prepare the plant to an impending attack (Bellés et al. 2008; Wei et al. 2013; Gargallo-Garriga et al. 2014). Knudsen et al. (2017) demonstrated that a flying moth recognizes its plant host based on the ratio between field-attractive and background VOCs embedded within a plant odour.

Interaction study between the volatile content in UC+PVY<sup>C</sup>-to, UC/Ma+PVY<sup>C</sup>-to and UC/Ma mock-inoculated plants was performed using HS-SPME/GC-MS at 28 dpi; a time-point in which the induction of tolerance mechanism against PVY<sup>C</sup>-to infection by grafting onto the tolerant Ma rootstock was already noticeable in the susceptible UC scion, since the recovery from the disease symptoms started to be observed at 14 dpi and fully visible by 21dpi (Spanò et al. 2020b). Thus, VOCs released by tomato plants in response to viral RNA accumulation and disease symptoms were correlated to the accumulation of viral RNA and disease symptoms estimated at 28 dpi by comparing the severely diseased non-grafted UC and the tolerant UC/Ma recovered from disease symptoms.

Overall, 111 VOCs emitted by tomato leaves in UC+PVY<sup>C</sup>-to, UC/Ma+PVY<sup>C</sup>-to and UC/Ma mock-inoculated plants were detected, and 107 volatile compounds were clearly identified, mainly belonging to terpenes, alcohols and methyl esters classes. These findings agree with the results of Niinemets et al. (2013) reporting the emission of C6 aldehydes, alcohols and derivatives, generally referred to as GLVs, in plants triggered by a biotic stress.

β-Phellandrene, Caryophyllene and 2-methyl-1-

**Table 5** Significant differential expression of infection-responsive volatile organic compounds (VOCs) genes in UC82 (UC) plants grafted onto Manduria (UC/Ma) vs. UC upon the infection recombinant strain of potato virus Y (PVY<sup>C</sup>-to)

Locus name	Gene function description	Fold change (FC) of UC/Ma+PVY <sup>C</sup> -to vs. UC+PVY <sup>C</sup> -to
<i>Solyc01g006560.2 (TomLoxF)</i>	Lipoxygenase	-1.43
<i>Solyc01g081340.2 (SI-SAMT)</i>	Salicylic acid carboxyl methyltransferase	-2.71
<i>Solyc07g006700.1 (CAP, PR1)</i>	CAP (Cysteine-rich secretory proteins, Antigen 5, and Pathogenesis-related 1 protein) superfamily protein	-2.24
<i>Solyc04g081550.2 (PR)</i>	Pathogenesis-related thaumatin superfamily protein	1.89
<i>Solyc04g064880.2 (PR)</i>	Pathogenesis-related family protein	-2.24
<i>Solyc01g097270.2 (PR4)</i>	Pathogenesis-related 4	2.19

Data are significantly differentially expressed genes (DEGs) with  $P \leq 0.05$ .

Pentanol were the most abundant compounds detected in all the samples analysed. Significantly different concentrations were detected for 34 out of the 107 total VOCs in virus-infected grafted plants UC/Ma compared to UC/Ma mock-inoculated, while 53 DVOCs were detected between non-grafted UC and UC/Ma plants upon infection by PVY<sup>C</sup>-to.

In tomato, six genes that encode various types of lipoxygenases (*TomloxA-F*) have been described (Mariutto et al. 2011). *TomloxF* encodes 13-LOX lipoxygenases, which are involved in the synthesis of oxylipins and play an important role in the response to biotic stress, such as pathogen attack (Dicke and Baldwin 2010; Howe and Jander 2018). *TomloxF* lipoxygenase participates in the biosynthesis of C5 and C6 GLVs compounds, such as 1-Penten-3-ol, 1-Penten-3-one, Pentanal, (Z)-2-Penten-1-ol, and 1-Pentanol, Hexanal, (Z)-3-Hexenal, 1-Hexanol, and (Z)-3-Hexen-1-ol). *TomloxF*, sharing 76% amino acid identity with *TomloxC*, is stimulated by the infection of *Pseudomonas putida* BTP1 to produce 13-HPOT and 13-hydroxy-octadecatrienoic acid (13-HOT) (Mariutto et al. 2011). Finally, GLVs possess fungicidal and bactericidal activity (Prost et al. 2005; Shiojiri et al. 2006b).

Since GLVs are released after infection with pathogenic fungi and bacteria (Croft et al. 1993; Heiden et al. 2003; Shiojiri et al. 2006a), this suggests a possible physiological role of these volatiles in limiting pathogen growth. Several observations support this hypothesis. For instance, upon infection with the pathogenic bacterium *P. syringae*, *Phaseolus vulgaris* (lima bean) leaves release relatively high amounts of the C6-aldehyde (E)-2-Hexenal and the C6-alcohol (Z)-3-Hexen 1-ol (Heiden et al. 2003). Moreover, pre-treatment with the C6-aldehyde (E)-2-Hexenal as well as genetic manipulation to enhance C6-volatile production, resulted in increased resistance against the necrotrophic fungus *Botrytis cinerea* in *Arabidopsis*, most likely as a result of both activation of defense responses and direct inhibition of fungal growth (Shiojiri et al. 2006b).

In our case, we dissected the tomato GLVs blend in the interaction of plants with the PVY<sup>C</sup>-to strain, necrogenic to tomato. Viral RNA accumulation and disease symptoms induced a significant emission of the short-chain alcohols, such as 2-methyl-1-Pentanol and 3-Pentanol, in non-grafted UC compared to UC/Ma.

Moreover, upon PVY<sup>C</sup>-to infection, there was a large increase in synthesis of all of the measured C6 volatiles, (E)-3-Hexen-1-ol, (E)-2-Hexen-1-ol and (E)-2-Hexenal, which are three of the most abundant GLVs emitted from susceptible infected UC tomatoes, as was also observed by Croft et al. (1993), and Heiden et al. (2003), where

*P. syringae* pv. *phaseolicola* infection provoked the emission of (Z)-3-Hexenol and (E)-2-Hexenal in bean and tobacco leaves, respectively. In tomato plants, (Z)-3-Hexenol, (Z)-3-Hexenal, and (Z)-3-Hexen 1-yl acetate were the dominant LOX products in the volatile emission after *B. cinerea* inoculation (Mariutto et al. 2011). The induction of (Z)-3-Hexenol and some of its derived compounds upon virus infection in tomato plants reported herein, extend GLVs emission to plant–virus interactions.

Volatile esters are also related to plant-to-plant signaling (Howe et al. 2018). The ester 3-Hexen-1-yl acetate is one of the most abundant volatiles emitted from pepper plants upon *Xanthomonas* infection (Dicke et al. 2010). In our virus–plant interaction, we observed an over production of 4-Hexen-1-yl acetate in non-grafted UC+PVY<sup>C</sup>-to plants in comparison to infected UC/Ma plants that showed milder symptoms.

Salicylic acid (SA), jasmonic acid (JA) and their methyl esters, methyl salicylate (MeSA) and methyl jasmonic acid (MeJA) respectively, are endogenous signal molecules that play essential roles in regulating abiotic and biotic stress responses in plants (Prost et al. 2005). SA accumulation is the classical signal molecule in incompatible interactions that accumulates at higher levels in virulent infections. The role of MeSA production was studied in indirect and direct defence responses of tomato to the spider mite *Tetranychus urticae* and to the root-invading fungus *Fusarium oxysporum* f. sp. *lycopersici*, respectively (Ament et al. 2010). In that study, spider mites induced the expression of salicylic acid methyl transferase (*SI-SAMT*), which led to the production of MeSA from SA, so that the induction of *SI-SAMT* is JA-dependent (Ament et al. 2010), suggested that crosstalk between JA and SA signalling pathways controlled the indirect defence response. Moreover, the silencing of the tomato *SI-SAMT* gene decreased the susceptibility to *F. oxysporum* f. sp. *lycopersici* and led to a major reduction in MeSA emission by plants. In our study, we detected enhanced MeSA emission after PVY<sup>C</sup>-to infection in diseased UC plants, suggesting the involvement of both SA and its methyl esters, MeSA, in the tomato defence response mechanisms to PVY<sup>C</sup>-to infection.

In order to verify whether the increase in VOCs detected upon PVY<sup>C</sup>-to infection was related to the production of specific VOCs biosynthesis machinery, the expression of infection-responsive *SI-SAMT* and *TomloxF* genes, involved in the *SI-SAMT* biosynthetic pathway of the MeSA, and implicated in the biosynthesis of GLVs, respectively, were retrieved from RNAseq analysis (Spanò et al. 2020b). We observed a positive correlation in the up-regulation of *TomloxF* and *SI-SAMT* genes at 14 dpi,



involved in GLVs and VOCs biosynthesis, respectively, with the differential emission of the corresponding VOCs at 28 dpi. This correlation suggests the maintenance of a defence response in infected plants is up to 28 dpi. The induction of the *TomloxF* gene has also been described by Mariutto *et al.* (2011), in tomato plants infected by *P. putida*, but this seems to be the first report of validation of the defensive role of this tomato LOX isoform as a result of infection caused by potyvirus in tomato plants.

## 5. Conclusion

The volatile profile emitted from the mock-inoculated grafted plants was chemically similar to that of the infected grafted plants tolerant against PVY<sup>C</sup>-to, but significantly different from the VOCs blend of infected tissues of the susceptible non-grafted UC variety. Our results show that PVY<sup>C</sup>-to infection induced qualitative and quantitative changes in host volatile emission in tomato plants and these changes depended on both PVY<sup>C</sup>-to RNA accumulation and disease symptoms developed. So far, most analyses of the VOCs emitted by tomato leaves have been performed under viral infections in non-grafted-host plants. To our knowledge, this is the first study in which the levels of all these signal molecules have been measured in grafted tomato plants infected by a potyvirus.

## Acknowledgements

We would like to thank Prof. D. Gallitelli from the University of Bari “Aldo Moro”, Italy for his help in the critical revision of the manuscript and helpful comments in preparing the manuscript. This study was carried out within the Agritech National Research Center, Italy, and received funding from the European Union NextGenerationEU (PIANO NAZIONALE DI RIPRESA E RESILIENZA (PNRR) – MISSIONE 4 COMPONENTE 2, INVESTIMENTO 1.4 – D.D. 1032 17/06/2022, CN00000022). This manuscript reflects only the authors' views and opinions, neither the European Union nor the European Commission can be considered responsible for them.

## Declaration of competing interest

The authors declare that they have no conflict of interest.

## References

Ament K, Krasikov V, Allmann S, Rep M, Takken F L W, Schuurink R C. 2010. Methyl salicylate production in tomato

- affects biotic interactions. *The Plant Journal*, **62**, 124–134.
- Anders S, Huber W. 2010. Differential expression analysis for sequence count data. *Genome Biology*, **11**, R106.
- Battaglia D, Bossi S, Cascone P, Digilio M C, Prieto J D, Fanti P, Guerrieri E, Iodice L, Lingua G, Lorito M, Maffei M E, Massa N, Ruocco M, Sasso R, Trotta V. 2013. Tomato below ground-above ground interactions: *Trichoderma longibrachiatum* affects the performance of *Macrosiphum euphorbiae* and its natural antagonists. *Molecular Plant–Microbe Interactions*, **26**, 1249–1256.
- Beck J J, Merrill G B, Higbee B S, Light D M, Gee W S. 2009. *In situ* seasonal study of the volatile production of almonds (*Prunus dulcis*) var. ‘Nonpareil’ and relationship to navel orangeworm. *Journal of Agricultural and Food Chemistry*, **57**, 3749–3753.
- Beck J J, Smith L, Merrill G B. 2008. *In situ* volatile collection, analysis, and comparison of three *Centaurea* species and their relationship to biocontrol with herbivorous insects. *Journal of Agricultural and Food Chemistry*, **56**, 2759–2764.
- Bellés J M, López-Gresa M P, Fayos J, Pallás V, Rodrigo I, Conejero V. 2008. Induction of cinnamate 4-hydroxylase and phenylpropanoids in virus-infected cucumber and melon plants. *Plant Science*, **174**, 524–533.
- Carr J P, Murphy A M, Tungadi T, Yoon J Y. 2019. Plant defense signals: Players and pawns in plant–virus–vector interactions. *Plant Science*, **279**, 87–95.
- Croft K P C, Juttner F, Slusarenko A J. 1993. Volatile products of the lipoxygenase pathway evolved from *Phaseolus vulgaris* (L.) leaves inoculated with *Pseudomonas syringae* pv. *phaseolicola*. *Plant Physiology*, **101**, 13–24.
- Deng H, Zhang Y, Reuss L, Suh J H, Yu Q, Liang G, Wang Y, Gmitter Jr F G. 2021. Comparative leaf volatile profiles of two contrasting mandarin cultivars against *Candidatus Liberibacter asiaticus* infection illustrate Huanglongbing tolerance mechanisms. *Journal of Agricultural and Food Chemistry*, **69**, 10869–10884.
- Dicke M, Baldwin I T. 2010. The evolutionary context for herbivore-induced plant volatiles: beyond the ‘cry for help’. *Trends in Plant Science*, **15**, 167–175.
- Dong X, Sun L, Maker G, Ren Y, Yu X. 2022. Ozone treatment increases the release of voc from barley, which modifies seed germination. *Journal of Agricultural and Food Chemistry*, **70**, 3127–3135.
- Eigenbrode S D, Bosque-Pérez N A, Davis T S. 2018. Insect-borne plant pathogens and their vectors: Ecology, evolution, and complex interactions. *Annual Review of Entomology*, **63**, 169–191.
- Erb M, Meldau S, Howe G A. 2012. Role of phytohormones in insect-specific plant reactions. *Trends in Plant Science*, **17**, 250–259.
- Gadhav K R, Gautam S, Rasmussen D A, Srinivasan R. 2020. Aphid transmission of *Potyvirus*: the largest plant-infecting RNA virus genus. *Viruses*, **12**, 773.
- Gaion L A, Braz L T, Carvalho R F. 2018. Grafting in vegetable

- crops: A great technique for agriculture. *International Journal of Vegetable Science*, **24**, 85–102.
- Gargallo-Garriga A, Sardans J, Pérez-Trujillo M, Rivas-Ubach A, Oravec M, Vecerova K, Urban O, Jentsch A, Kreyling J, Beierkuhnlein C, Parella T, Peñuelas J. 2014. Opposite metabolic responses of shoots and roots to drought. *Scientific Reports*, **4**, 1–17.
- Groen S C, Jiang S, Murphy A M, Cunniffe N J, Westwood J H, Davey M P, Bruce T J A, Caulfield J C, Furzer O J, Reed A, Robinson S I, Miller E, Davis C N, Pickett J A, Whitney H M, Glover B J, Carr J P. 2016. Virus infection of plants alters pollinator preference: A payback for susceptible hosts? *PLoS Pathogens*, **12**, e1005790.
- Heiden A C, Kobel K, Langebartels C, Schuh-Thomas G, Wildt J. 2003. Emissions of oxygenated volatile organic compounds from plants part i: Emissions from lipoxygenase activity. *Journal of Atmospheric Chemistry*, **45**, 143–172.
- Howe G A, Jander G. 2018. Plant immunity to insect herbivores. *Annual Review of Plant Biology*, **59**, 41–66.
- Hull R. 2014. *Plant Virology*. 5th ed. In: Hull R, ed., Academic Press, London, UK.
- Kim D, Langmead B, Salzberg S L. 2015. HISAT: A fast spliced aligner with low memory requirements. *Nature Methods*, **12**, 357–360.
- Knudsen G K, Norli H R, Tasin M. 2017. The ratio between field attractive and background volatiles encodes host-plant recognition in a specialist moth. *Frontiers in Plant Science*, **8**, 2206.
- Kørner J, Pitzalis N, Peña E J, Erhardt M, Vazquez F, Heinlein M. 2018. Crosstalk between PTGS and TGS pathways in natural antiviral immunity and disease recovery. *Nature Plants*, **4**, 157–164.
- Kumar S, Bharti N, Saravaiya S N. 2018. Vegetable grafting: A surgical approach to combat biotic and abiotic stresses: A review. *Agricultural Reviews*, **39**, 1–11.
- Langmead B, Trapnell C, Pop M, Salzberg S L. 2009. Ultrafast and memory-efficient alignment of short DNA sequences to the human genome. *Genome Biology*, **10**, 1–10.
- Lin Y, Huang J, Akutse K, Hou Y. 2022. Phytopathogens increase the preference of insect vectors to volatiles emitted by healthy host plants. *Journal of Agricultural and Food Chemistry*, **70**, 5262–5269.
- López-Berenguer C, Donaire L, González-Ibeas D, Gómez-Aix C, Truniger V, Pechar G S, Aranda M A. 2021. Virus-infected melon plants emit volatiles that induce gene deregulation in neighboring healthy plants. *Phytopathology*, **111**, 862–869.
- Mariutto M, Duby F, Adam A, Bureau C, Fauconnier M L, Ongena M, Thonart P, Dommes J. 2011. The elicitation of a systemic resistance by *Pseudomonas putida* BTP1 in tomato involves the stimulation of two lipoxygenase isoforms. *BMC Plant Biology*, **11**, 1–15.
- Mascia T, Finetti-Sialer M M, Cillo F, Gallitelli D. 2010a. Biological and molecular characterization of a recombinant isolate of *Potato virus Y* associated with a tomato necrotic disease occurring in Italy. *Journal of Plant Pathology*, **9**, 131–138.
- Mascia T, Santovito E, Gallitelli D, Cillo F. 2010b. Evaluation of reference genes for quantitative reverse-transcription polymerase chain reaction normalization in infected tomato plants. *Molecular Plant Pathology*, **11**, 805–816.
- Mauck K E, Bosque-Pérez N A, Eigenbrode S D, De Moraes C, Mescher M C. 2012. Transmission mechanisms shape pathogen effects on host–vector interactions: evidence from plant viruses. *Functional Ecology*, **26**, 1162–1175.
- Minutillo S A, Mascia T, Gallitelli D. 2012. A DNA probe mix for the multiplex detection of ten artichoke viruses. *European Journal of Plant Pathology*, **134**, 459–465.
- Mudge K, Janick J, Scofield S, Goldschmidt E E. 2009. A history of grafting. In: Janick J, ed., *Horticultural Reviews*. John Wiley & Sons, NY, USA. pp. 435, 437–493.
- Niinemets U, Kännaste A, Copolovici L. 2013. Quantitative patterns between plant volatile emissions induced by biotic stresses and the degree of damage. *Frontiers in Plant Science*, **4**, 262.
- Prost I, Dhondt S, Rothe G, Vicente J, Rodriguez M J, Kift N, Carbonne F, Griffiths G, Esquerré-Tugayé M T, Rosahl S, Castresana C, Hamberg M, Fournier J. 2005. Evaluation of the antimicrobial activities of plant oxylipins supports their involvement in defense against pathogens. *Plant Physiology*, **139**, 1902–1913.
- Scholthof K B G, Adkins S, Czosnek H, Palukaitis P, Jacquot E, Hohn T, Hohn B, Saunders K, Candresse T, Ahlquist P, Hemenway C, Foster G D. 2011. Top 10 plant viruses in molecular plant pathology. *Molecular Plant Pathology*, **12**, 938–954.
- Sharma R, Zhou M, Hunter M D, Fan X. 2019. Rapid *in situ* analysis of plant emission for disease diagnosis using a portable gas chromatography device. *Journal of Agricultural and Food Chemistry*, **67**, 7530–7537.
- Shiojiri K, Kishimoto K, Ozawa R, Kugimiya S, Urashimo S, Arimura G, Horiuchi J, Nishioka T, Matsui K, Takabayashi J. 2006a. Changing green leaf volatile biosynthesis in plants: An approach for improving plant resistance against both herbivores and pathogens. *Proceedings of the National Academy of Sciences of the United States of America*, **103**, 16672–16676.
- Shiojiri K, Ozawa R, Matsui K, Kishimoto K, Kugimiya S, Takabayashi J. 2006b. Role of the lipoxygenase/lyase pathway of host-food plants in the host searching behaviour of two parasitoid species, *Cotesia glomerata* and *Cotesia plutellae*. *Journal of Chemical Ecology*, **32**, 969–979.
- Spanò R, Ferrara M, Gallitelli D, Mascia T. 2020a. The role of grafting in the resistance of tomato to virus. *Plants*, **9**, 1042–1062.
- Spanò R, Ferrara M, Montemurro C, Mulè G, Gallitelli D, Mascia T. 2020b. Grafting alters tomato transcriptome and enhances tolerance to an airborne virus infection. *Scientific Reports*, **10**, 1–13.

- Spanò R, Mascia T, Kormelink R, Gallitelli D. 2015. Grafting on a non-transgenic tolerant tomato variety confers resistance to the infection of a Sw5-breaking strain of tomato spotted wilt virus via RNA silencing. *PLoS ONE*, **10**, e0141319.
- De Vos M, Jander G. 2010. Volatile communication in plant–aphid interactions. *Current Opinion in Plant Biology*, **13**, 366–371.
- Wei J, Yan L, Ren QIN, Li C, Ge F, Kang L E. 2013. Antagonism between herbivore-induced plant volatiles and trichomes affects tritrophic interactions. *Plant, Cell & Environment*, **36**, 315–327.
- Wylie S J, Adams M, Chalam C, Kreuze J, López-Moya J J, Ohshima K, Praveen S, Rabenstein F, Stenger D, Wang A, Zerbini F M, ICTV Report Consortium. 2017. ICTV virus taxonomy profile: Potyviridae. *Journal of General Virology*, **98**, 352–354.
- Zellner B D, Bicchi C, Dugo P, Rubiolo P, Dugo G, Mondello L. 2008. Linear retention indices in gas chromatographic analysis: A review. *Flavour and Fragrance Journal*, **23**, 297–314.

Executive Editor-in-Chief WAN Fang-hao  
Managing Editor ZHANG Juan